RESEARCH ARTICLE | MARCH 18 2026

Scenarios with predominant heating of electrons and ions in Wendelstein 7-X

Ya. I. Kolesnichenko ; V. V. Lutsenko ; A. V. Tykhyy ; W7-X Team

Phys. Plasmas 33, 032506 (2026)
https://doi.org/10.1063/5.0315228

Physics of Plasmas ARTICLE pubs.aip.org/aip/pop

Scenarios with predominant heating of electrons and ions in Wendelstein 7-X

Cite as: Phys. Plasmas **33**, 032506 (2026); doi: 10.1063/5.0315228
Submitted: 4 December 2025 · Accepted: 28 February 2026 ·
Published Online: 18 March 2026

View Online Export Citation CrossMark

Ya. I. Kolesnichenko, V. V. Lutsenko, A. V. Tykhyy,[a] and W7-X Team[b]

AFFILIATIONS

Institute for Nuclear Research, Prospekt Nauky 47, Kyiv 03028, Ukraine

[a]Author to whom correspondence should be addressed: tykhyy@kinr.kiev.ua
[b]See author list of Grulke *et al.*, Nucl. Fusion **64**, 112002 (2024).

ABSTRACT

Using a 0D paradigm for energy balance equations, it is shown that in plasmas with predominant electron heating, in particular, during electron cyclotron resonance heating, the ion temperature is always capped (restricted) by a temperature below the electron temperature. When ion thermal conductivity is anomalous (e.g., due to turbulence caused by the ion temperature gradient (ITG) instability) the capping can have features of the ion temperature clamping observed in stellarators and tokamaks, in particular, in the Wendelstein 7-X stellarator, which is the focus of this paper. Therefore, the used paradigm can serve as a tool for the description of the clamping. Relations are obtained, which can be used for diagnostics of the plasma energy confinement time during the clamping. Employing the same paradigm, plasmas heated by neutral beam injection (NBI) are considered, with the aim of investigating the possibility of achieving a steady state ion temperature exceeding the electron one ($T_i > T_e$) in W7-X. It is revealed that in the steady state, the fraction of NBI power received by the bulk plasma ions has a maximum at a certain electron temperature, $3-4$ keV, when protons with the maximum energy 55 keV are injected into a hydrogen plasma. This tends to break the necessary condition for $T_i > T_e$ obtained in this work, i.e., the heating rate of the electrons should be less than their energy loss rate. Nevertheless, steady state scenarios with $T_i > T_e$ are possible at least in plasmas with relatively low density and sufficiently high energy confinement time of the ions (when ITG turbulence is absent or mitigated).

I. INTRODUCTION

A peculiarity of the Wendelstein 7-X stellarator is that the neoclassical transport in it is rather low. Therefore, it almost does not affect plasma confinement, which is determined mainly by turbulence, as in tokamaks.[1] Applying ECRH (electron cyclotron resonance heating), plasmas with electron temperatures in the range $1-7$ keV were obtained.[2] However, ion temperature was considerably less than 7 keV; moreover, ion temperature clamping at $T_i \sim 1.5$ keV was revealed.[3] This is not an evidence of a drawback of the magnetic configuration of Wendelstein 7-X (and W7-X has even a certain advantage due to the existence of a "stability valley" in maximum-J stellarators, where electrostatic instabilities are suppressed[4]). Turbulence arises because of plasma micro-instabilities which are driven by spatial gradients of plasma parameters. Therefore, it is not surprising that this phenomenon was also observed in tokamaks.[5,6]

An important role belongs to the ion temperature gradient (ITG) instability, which leads to degradation of the ion energy confinement time.[7] Theory predicts that the ITG threshold $\eta_{i,cr}$ ($\eta_i \equiv d\ln T_i/d\ln n_i$, where T_i and n_i are the ion temperature and density, respectively) increases when $T_i > T_e$,[8] so that potentially plasmas with $T_i > T_e$ are more stable with respect to ITG. In experiments on the LHD stellarator, transition from the ITG-dominant case to the stable ITG case is observed as the formation of an ion internal transport barrier (ITB). When $T_i/T_e < 1$, no ITB is formed, or the ITB is terminated.[9,10] A similar T_i/T_e ratio effect on global confinement time was reported in the EAST tokamak.[11] The regime with $T_i > T_e$ is also beneficial because it provides higher fusion reactivity for the same β (the ratio of plasma pressure to the magnetic field pressure) and plasma density.

Plasmas with $T_i \gtrsim T_e$ occurred in tokamaks, in particular, in JET and TFTR. The most exciting result was achieved in the TFTR supershot experiment, where $T_i/T_e = 3$ with $T_i = 35$ keV took place.[12] In the core region, $r/a \leq 0.3$, transport diffusivity coefficients were considerably smaller than those in L-mode plasmas, as shown in Fig. 5 of Ref. 13, and $\eta_i(r)$ was below the ITG threshold (see Fig. 1).

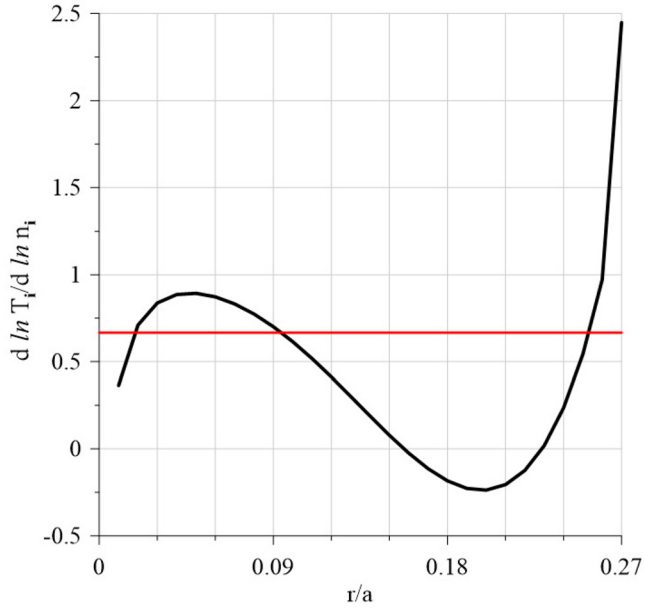

FIG. 1. The parameter $\eta_i = d\ln T_i/d\ln n_i$ in the TFTR supershot (black curve) and the ITG instability threshold (red line $\eta_{cr} = 2/3$[14]) vs r/a. Calculations were carried out for the parameters shown in Fig. 3 of Ref. 12; reliable flux surface averaged parameters were available only for $r/a < 0.27$, which explains why $\eta_i(r)$ is shown in the region $r/a \leq 0.27$. We observe that the black curve lies below the red line in the region $0.09 \leq r/a \leq 0.25$. Moreover, the analysis in Ref. 8, based on two-fluid hydrodynamics presented in Ref. 15, leads to $\eta_{cr} > 2/3$. This indicates that ITG turbulence did not arise in the plasma core.

This work aims to contribute, first, to the understanding of the physics of ion temperature clamping and, second, to the study of conditions of regimes with $T_i > T_e$. Special attention is paid to W7-X. The analysis is based on a 0D paradigm of plasma energy balance. This approach has the advantage of being simple, and at the same time, generic because the equations used are valid for any transport coefficients. It may provide insight not provided by the standard codes used for modeling particular discharges. Moreover, it enables one to describe plasma heating by ECRH, neutral beam injection (NBI), and ion cyclotron resonance heating (ICRH) on the same footing.

The structure of the work is as follows. Section II analyzes equations of the energy balance of the ion and electron components without specifying plasma parameters. It consists of Subsections II A–II C. Subsection II A presents the equations used in this work. Subsection II B considers plasmas with ECRH; it aims to find conditions leading to ion temperature clamping. Energy balance in plasmas with NBI heating is studied in Sec. II C, with emphasis on possible regimes with $T_i > T_e$. Section III is devoted to Wendelstein 7-X. In Subsection III A, the relations obtained in Sec. II B are applied to ECRH plasmas in W7-X. Subsections III B and III C deal with NBI heating in W7-X: the fraction of NBI power delivered to the ions, f_i, in W7-X is studied, and predictive calculations are carried out. In addition, the work contains two Appendixes. Relations for f_i are derived in Appendix A. The stability of solutions of the steady state energy balance equation is considered in Appendix B. The results of the work are summarized and discussed in Sec. IV.

II. GENERAL CONSIDERATION

A. Basic equations

We consider a two-component plasma heated by the injection of particles (NBI) and an RF field. It will be described by the following steady-state equations for the temperatures of ions and electrons, which take into account plasma heating by external sources, energy exchange between electrons and ions, and energy losses:

$$\frac{3}{2}\frac{dT_i}{dt} = p_H f_i - \nu_{ei}(T_i - T_e) - \frac{3T_i}{2\tau_{Ei}} = 0, \tag{1}$$

$$\frac{3}{2}\frac{dT_e}{dt} = p_H f_e + \nu_{ei}(T_i - T_e) - \frac{3T_e}{2\tau_{Ee}} = 0. \tag{2}$$

Here, the subscripts e and i label electrons and ions, respectively; p_H is the specific power, i.e., the power of plasma heating by NBI and RF field related to one particle, f_j with $j = e,\ i$ is the fraction of the injected energy deposited to the j-component of the plasma, ν_{ei} is the collision frequency of energy exchange between electrons and ions, and τ_{Ee} and τ_{Ei} are the energy confinement times (which are determined by diffusivity and radiation).

These equations describe the core plasma region; they are not relevant to processes associated with divertor, plasma detachment etc. In this region energy losses due to radiation are small compared to those near the plasma edge, see, e.g., Ref. 3.

Equations (1) and (2) can be written in other forms. First, combining them we have

$$p_H = \frac{3}{2}\left(\frac{T_i}{\tau_{Ei}} + \frac{T_e}{\tau_{Ee}}\right), \tag{3}$$

$$p_H(f_i - f_e) + 2\nu_{ei}(T_e - T_i) = \frac{3}{2}\left(\frac{T_i}{\tau_{Ei}} - \frac{T_e}{\tau_{Ee}}\right). \tag{4}$$

Second, when T_i is eliminated by introducing $\Theta \equiv T_i/T_e$, they look as follows:

$$\frac{2}{3}\frac{p_H\tau_{Ee}}{T_e} = \frac{\Theta\tau_{Ee}}{\tau_{Ei}} + 1, \tag{5}$$

$$\Theta\left(1 + \frac{0.75}{\tau_{Ei}\nu_{ei}}\right) = \delta_f + 1 + \frac{0.75}{\tau_{Ee}\nu_{ei}}, \tag{6}$$

where

$$\delta_f = \frac{p_H}{\nu_{ei}}\frac{(f_i - f_e)}{2T_e}. \tag{7}$$

Explicit forms of ν_{ei} and p_H are given below.

The frequency of energy exchange between electrons and ions is

$$\nu_{ei} = \frac{3M_e n_e}{M_i n_i}\frac{1}{\tau_e} = \frac{4\sqrt{2\pi}\lambda e^4 Z_i^2 n_e\sqrt{M_e}}{M_i T_e^{3/2}}$$

$$= 1.5\lambda_{ei} n_{19}\frac{Z_i^2}{A_i T_{e,keV}^{3/2}} s^{-1}, \tag{8}$$

where τ_e is the electron–ion collision time, $T_{e,keV}$ the electron temperature in keV, $n_{19} = n_i/(10^{19}\mathrm{m}^{-3})$ the normalized ion density in m^{-3}, A_i the ion mass number, Z_i the ion charge number, $M_{e,i}$ the electron/ion mass, and λ_{ei} the Coulomb logarithm. The specific power is

$$p_H = \frac{\mathcal{P}}{n_e V_p} = \frac{10^3 \mathcal{P}_{MW}}{1.6 n_{19} V_p} \text{keV/s}, \tag{9}$$

where V_p is the plasma volume in m^3, and $\mathcal{P} = P_{nbi} + \mathcal{P}_{RF}$ is the total heating power.

Other useful relations are

$$\frac{p_H}{\nu_{ei}} = 416.7 \frac{A_i \mathcal{P}_{MW} T_{e,keV}^{3/2}}{Z_i^2 n_{19}^2 V_p \lambda_{ei}} \text{keV}, \tag{10}$$

and

$$H \equiv \frac{p_H}{\nu_{ei} T_{e,keV}} = 416.7 \frac{A_i \mathcal{P}_{MW} \sqrt{T_{e,keV}}}{Z_i^2 n_{19}^2 V_p \lambda_{ei}}. \tag{11}$$

The energy spectrum of NBI ions has sharp maxima at $\mathcal{E}_0$, $\mathcal{E}_0/2$, and $\mathcal{E}_0/3$. Therefore, the electron/ion power fraction is

$$f_i = \sum_{\sigma=1}^{3} \frac{\mathcal{P}_\sigma}{\mathcal{P}} f_\sigma^i(\mathcal{E}_\sigma) + \frac{\mathcal{P}_{RF}}{\mathcal{P}} f_{RF}^i, \quad f_e = 1 - f_i, \tag{12}$$

where $\mathcal{P}_\sigma$ is the NBI power with the particle energy $\mathcal{E}_\sigma$.

B. Capping T_i below T_e

Let us assume that f_i is small,

$$f_i \ll \frac{1.5 T_i}{p_H \tau_{Ei}}. \tag{13}$$

In this case, ions are mainly heated due to energy exchange with electrons. In particular, this is the case in discharges with ECRH (where $f_i = 0$). When Eq. (13) is satisfied and the f_i term is neglected, Eq. (1) reduces to

$$\frac{T_i}{T_e} = \frac{1}{1+\alpha}, \tag{14}$$

where $\alpha = 1.5(\nu_{ei}\tau_{Ei})^{-1}$. This equation shows that T_i is always less than T_e, which means that during ECRH T_i is always capped (restricted, constrained) by a temperature below T_e.

Because $\alpha \propto \tau_{Ei}$, when the ion heat conductivity is anomalous, e.g., due to ITG turbulence, the capping is anomalous, too. The anomalous ion heat conductivity decreases the energy confinement time, decreasing the coupling of ions with electrons (α grows). This decreases the ratio T_i/T_e, exacerbating stiffness of the ion profile, cf. Refs. 16 and 17. Because during ECRH only electrons receive the energy ($f_i = 0$), we have $\max\{T_i^{itg}\} < \max\{T_i^{neo}\}$, where subscripts "itg" and "neo" label plasmas with ITG turbulence and with neoclassical transport, respectively. This agrees with Fig. 1 in Ref. 3, which shows that experimentally observed ion temperature in a W7-X discharge with clamping is less than that calculated using neoclassical transport coefficients.

Below, we investigate other features of anomalous capping to see whether and when they correspond to those of the ion temperature clamping described in Ref. 3.

First of all, we note that the ion temperature is close to T_e for $\alpha \ll 1$, i.e., when

$$\tau_{Ei}\nu_{ei} \gg 1. \tag{15}$$

This equation provides the best result of ECRH in the sense that T_i is maximum possible for the achieved T_e. Let us assume that it is fulfilled at a certain temperature T_c (then $T_e \approx T_i \approx T_c$) due to a certain specific heating power p_{Hc}. A question then arises as to what will happen if specific power increased (either due to greater ECRH power or lower plasma density), so that $p_H > p_{Hc}$. Looking at Eq. (2) and taking into account that $T_e > T_i$, we conclude that T_e will increase. Because $\nu_{ei} \propto n_e T_e^{-3/2}$, this will increase α and the ratio T_e/T_i according to Eq. (14). Thus, the increase in T_e leads to the growth of T_e/T_i.

To obtain the capped temperature, we write Eq. (14) as

$$T_i = \frac{1}{1+\alpha} T_e, \tag{16}$$

where $\alpha = \alpha(T_e, T_i)$. We obtain from here

$$\frac{dT_i}{dT_e} = \frac{1 - \alpha_e' T_e/(1+\alpha)}{1 + \alpha + \alpha_i' T_i}, \tag{17}$$

where $\alpha_j' = \partial\alpha/\partial T_j$, normally $\alpha_j' > 0$, $j = e, i$. We conclude that $dT_i/dT_e > 0$ when $1 + \alpha > \alpha_e' T_e$, $dT_i/dT_e < 0$ when $1 + \alpha < \alpha_e' T_e$, and $dT_j/dT_e = 0$ when

$$1 + \alpha = \alpha_e' T_e. \tag{18}$$

If these conditions are fulfilled, $T_i(T_e)$ has a maximum at a certain α_* determined by Eq. (18). This implies that T_i is capped at α_*.

To be more specific, we take $\alpha \propto T_e^{\mu+1.5} T_i^\nu$ with $\mu > 0$, $\nu > 0$. Then $dT_i/dT_e \geq 0$ provided

$$\alpha \leq \frac{1}{\mu + 0.5}. \tag{19}$$

This means that $T_i(\alpha)$ is growing in the region $\alpha_{min} \leq \alpha < (\mu + 0.5)^{-1}$, with $\alpha_{min} = \alpha(T_c)$, reaching its maximum at $\alpha_* = (\mu + 0.5)^{-1}$ where

$$\frac{T_{i*}}{T_{e*}} = 1 - \bar{\mu}^{-1} = \frac{\mu + 0.5}{\mu + 1.5}. \tag{20}$$

In the region $\alpha > \alpha_*$ the ratio T_{i*}/T_{e*} decreases. Hence, stronger heating increases T_e but decreases T_i.

At the point of maximum ion temperature, we can write $\alpha_* = C T_{e*}^{\bar{\mu}} T_{i*}^\nu$, with $\bar{\mu} = \mu + 1.5$ and $C(T_{e*}, T_{i*}) = \text{const}$. Using this relation and that $\alpha_* = (\bar{\mu} - 1)^{-1}$ we obtain the following electron temperature at the point where T_i is maximum:

$$T_{e*} = \left(\frac{1}{C T_{i*}^\nu (\bar{\mu} - 1)} \right)^{1/\bar{\mu}}. \tag{21}$$

Because of this relation, we can eliminate T_e in Eq. (16) and obtain maximum T_i

$$T_{i*} = \left[\frac{1}{C} \frac{1}{\bar{\mu}^{\bar{\mu}}} (\bar{\mu} - 1)^{\bar{\mu}-1} \right]^{1/(\bar{\mu}+\nu)}, \tag{22}$$

where $C = C(n)$ being determined by $\nu_{ei}(n)$ and $\tau_{Ei}(n)$.

This T_{i*} does not depend on the heating power. In addition, it weakly depends on the plasma density provided

$$\mu + \nu + 1.5 \gg 1, \tag{23}$$

which is presumably the case during ITG turbulence. To see this, we note that $T_{i*} \propto C^{1/(\mu+\nu+1.5)}$, which weakly depends on C provided

that Eq. (23) is satisfied. For instance, when C changes by a factor of 3, $T_{i*2}/T_{i*1} = 1.3$ for $\mu + \nu = 2.5$.

The clamping experiments on W7-X show that the maximum of $T_i(T_e)$ is soft. To see whether and when this can be the case, we calculate the second derivative d^2T_i/dT_e^2 at T_{e*}

$$T_e \frac{d^2T_i}{dT_e^2}\bigg|_{\alpha_*} = -\frac{(\mu + 0.5)^2}{\mu + \nu + 1.5}. \tag{24}$$

It follows from here that the maximum of $T_i(T_e)$ is soft when $\nu + 1.25 > \mu^2$. This suggests that the anomalous ion transport should depend on T_i stronger than on T_e.

Thus, all ingredients of the clamping can be consistent with predictions of the 0D paradigm.

Because the maximum of $T_i(T_e)$ is soft during the clamping, it is reasonable to approximate the maximum temperature by T_c and employ equation

$$\frac{2}{3}\nu_{ei}\tau_{Ei}T_e(1 - \Theta) = T_i \approx T_c, \qquad \text{where } \Theta \ll 1. \tag{25}$$

Now we proceed to Eq. (2), writing it with $f_e = 1$ as follows:

$$p_H - \frac{3T_e}{2\tau_{Ee}} = \nu_{ei}T_e(1 - \Theta). \tag{26}$$

Let us consider this equation in the assumption that the specific power well exceeds p_{Hc}, so that

$$\frac{p_H}{\nu_{ei}T_e} \gg 1 - \Theta, \tag{27}$$

for any $\Theta < 1$. In this case, the RHS in Eq. (26) can be neglected, i.e., the electron–ion coupling is small. Then, Eq. (26) reduces to

$$p_H \approx \frac{1.5T_e}{\tau_{Ee}}. \tag{28}$$

Because of this equation and Eqs. (14) and (27), we can write

$$\frac{1.5T_e}{\tau_{Ee}} \approx p_H \gg \nu_{ei}(T_e - T_i) = 1.5\frac{T_i}{\tau_{Ei}}. \tag{29}$$

It follows from this that when Eq. (15) is not satisfied, and therefore Θ is not close to unity, we have

$$\frac{T_e}{T_i} \gg \frac{\tau_{Ee}}{\tau_{Ei}}. \tag{30}$$

This means that $T_e \gg T_i$ when $\tau_{Ei} \le \tau_{Ee}$ (confinement of ion energy does not exceed that of the electrons), and thus, the clamping of T_i clearly manifests. In contrast, Eq. (30) actually does not restrict T_i/T_e when $\tau_{Ei} \gg \tau_{Ee}$.

Thus, the clamping arises in the presence of ITG turbulence or other turbulence, deteriorating the ion energy confinement time. In plasmas with clamping, there exists a steady state with $T_i \approx T_e$ (which requires $\tau_{Ei}\nu_{ei} \gg 1$) and $\tau_{Ei} \le \tau_{Ee}$. Increasing specific power above p_{Hc} (i.e., increasing the heating power or decreasing the particle density and /or plasma volume) increases the ratio T_e/T_c, making the electron temperature higher but weakly changing T_i. The clamping temperature T_c is approximately determined by Eq. (3) with minimum specific power providing $T_i \approx T_e$. This equation due to $T_e = T_i$ and $\tau_{Ei} < \tau_{Ee}$ reads

$$p_{Hc} = 1.5\frac{T_c}{\tau_E}, \qquad \text{with} \qquad \tau_E = (\tau_{Ei}^{-1} + \tau_{Ee}^{-1})^{-1} \sim \tau_{Ei}, \tag{31}$$

where τ_E is determined mainly by thermal conductivity and plasma radius. Note that Eq. (31) can be used for diagnostics; knowing T_c and p_{Hc} from experiment, one can calculate τ_E. In experiments with $p_H \gg p_{Hc}$, τ_{Ei} can be calculated by means of Eq. (25).

ECRH represents a limit case of energy transfer from the heating system to the ions, $f_i = 0$. When $f_i \neq 0$ but small enough to satisfy Eq. (13), clamping still can occur. However, when Eq. (13) breaks, the heating term $p_H f_i$ in Eq. (1) becomes non-negligible and therefore the clamping effect disappears. This can take place when ECRH is accompanied by simultaneous plasma heating by ICRH/NBI.

C. Removing restriction for T_i

It immediately follows from Eq. (2) for electrons that scenarios with high ion temperature in the steady state ($T_i > T_e$) are possible only when electron heating by external sources is less than the electron energy loss rate:

$$p_H f_e < \frac{1.5T_e}{\tau_{Ee}}. \tag{32}$$

On the other hand, it follows from Eq. (5) that $\Theta > 1$ provided:

$$p_H\tau_{Ee} > 1.5T_e \max\left\{1, \frac{\tau_{Ee}\Theta}{\tau_{Ei}}\right\}. \tag{33}$$

When $\Theta\tau_{Ee} > \tau_{Ei}$, Eqs. (33) and (32) are self-consistent provided that

$$f_e < \frac{\tau_{Ei}}{\Theta\tau_{Ee}} < 1. \tag{34}$$

In the contrary case, $\Theta\tau_{Ee} < \tau_{Ei}$

$$f_e < 1. \tag{35}$$

To see Θ for any ratio of f_i/f_e we write Eq. (6) as follows:

$$\Theta = \frac{1 + 0.75(\tau_{Ee}\nu_{ei})^{-1} + \delta_f}{1 + 0.75(\tau_{Ei}\nu_{ei})^{-1}}, \tag{36}$$

where $\delta_f \propto (f_i - f_e)$ is given by Eq. (7). We observe that $f_i > f_e$ ($\delta_f > 0$) tends to provide $\Theta > 1$, but the effect is considerable when $\delta_f > 1$, i.e.,

$$208\frac{A_i\mathcal{P}_{MW}T_{e,keV}^{1/2}}{Z_i^2 n_{19}^2 V_p \lambda_{ei}}(f_i - f_e) > 1. \tag{37}$$

When electron–ion coupling is weak, a "hot-ion mode," i.e., $T_i \gg T_e$, is possible. The necessary conditions are

$$\nu_{ei}\tau_{Ei} \ll 1.5 \tag{38}$$

and

$$\nu_{ei}\tau_{Ee}\Theta \ll 1.5. \tag{39}$$

Then

$$\Theta = \frac{f_i\tau_{Ei}}{f_e\tau_{Ee}}, \tag{40}$$

which well exceeds unity for

$$f_i\tau_{Ei} \gg f_e\tau_{Ee}. \tag{41}$$

In the case of $f_e = 0$, or at least, $f_e \ll 1.5T_e/(p_H\tau_{Ee})$

$$\Theta = \frac{1.5}{\nu_{ei}\tau_{Ee}} + 1. \tag{42}$$

III. APPLICATION TO W7-X

A. ECRH

Relations for the ion temperature capping were obtained in Sec. II B. It was concluded that the features of capping can be the same as those of clamping when certain conditions are fulfilled. Here, we consider whether this conclusion agrees with experimental observations in W7-X.

The dependence of T_i on T_e, which is determined by Eq. (14) for $\alpha = CT_e^{\mu+1.5}T_i^{\nu}$ with $\mu = 1/2$, $\nu = 2$, is shown in Fig. 2 (left panel) by solid red and blue lines for low particle density and high particle density, respectively. The constant C was selected to encompass experimental data points in various W7-X discharges while providing $T_e \approx T_i$ at high density: $C = 0.12$ for low density $n_{19} = 3$ (red line), $C = 0.031$ for high density $n_{19} = 12$ (blue line), which corresponds to $\tau_{Ei} = 0.15T_{e,keV}^{-1/2}T_{i,keV}^{-2}(\mathrm{s})$. It is worth mentioning that the blue solid line in the region $T_e \gg 1$ keV corresponds to heating power that well exceeds that in the W7-X experiments. To see this, let us consider an example with $n_{19} = 12$, $T_e = 6$ keV, and $T_i = 1.5$ keV. Using Eq. (3), we obtain

$$\mathcal{P} = V_p n_e T_i\left(\frac{1}{\tau_{Ei}} + \frac{4}{\tau_{Ee}}\right). \tag{43}$$

For a given T_e and a small change of the ion temperature $\Delta T_i \ll T_i$ determined by the distance from the blue curve to the upper border of the yellow area, Eq. (43) reduces to

$$\frac{\mathcal{P}_1}{\mathcal{P}_2} \approx \frac{n_{e1}}{n_{e2}} = \frac{12}{2.5} = 4.8, \tag{44}$$

where subscripts 1 and 2 label the points on the blue curve and the top of the yellow area at $T_e = 6$ keV, $n_{e1} = 12$, and $n_{e2} = 2.5$. Thus, in the considered example with a prescribed $T_e \gg T_i$, a small increase in the ion temperature compared to that observed experimentally requires a strong increase in the heating power. This result, while paradoxical at first sight, has a simple explanation: the large ratio of T_e/T_i achieved due to the ion clamping took place in plasmas with low density, whereas the calculated upper curve employed a high particle density. The "paradox" arises because the particle density is not shown in Fig. 2 (left panel); it disappears in the 3D figure shown in the right panel of Fig. 2. Thus, the blue line requires unrealistically large heating power for $T_e \gg T_i$ (but not for $T_e \approx T_i$).

The dependence of T_e and T_i on the plasma density is shown in Fig. 3. T_e was determined by Eq. (28) because the maximum heating power, $\mathcal{P} = 7$ MW, was sufficiently large. Electron energy confinement time was taken to be $\tau_{Ee} = 0.13$ s, which corresponds to $\chi_e = 0.5\mathrm{m}^2/\mathrm{s}$.[17] T_i was determined from T_e using Eq. (14) with the same parameters as in Fig. 2. The use of Eq. (28) is justified when the condition (27) is fulfilled. In this case, (27) is satisfied for high ECRH power and low density even with small Θ. For higher densities, Θ approaches unity and (27) becomes insensitive to density. The results of these calculations lie in the region of experimental observations.

The results shown in Figs. 2 and 3 demonstrate that the used 0D model can describe the bulk of experimental data in discharges with and without ion clamping. Below, we consider particular W7-X discharges.

Conditions of the appearance and absence of the ion-temperature clamping were found in Sec. II B. Below, we consider their fulfillment in W7-X.

First, we examine discharges from the OP2.1 campaign presented in Ref. 17. In discharge W7X20180920.013 (Fig. 1 of Ref. 17), with a hydrogen plasma, standard magnetic configuration, and 4.7 MW of

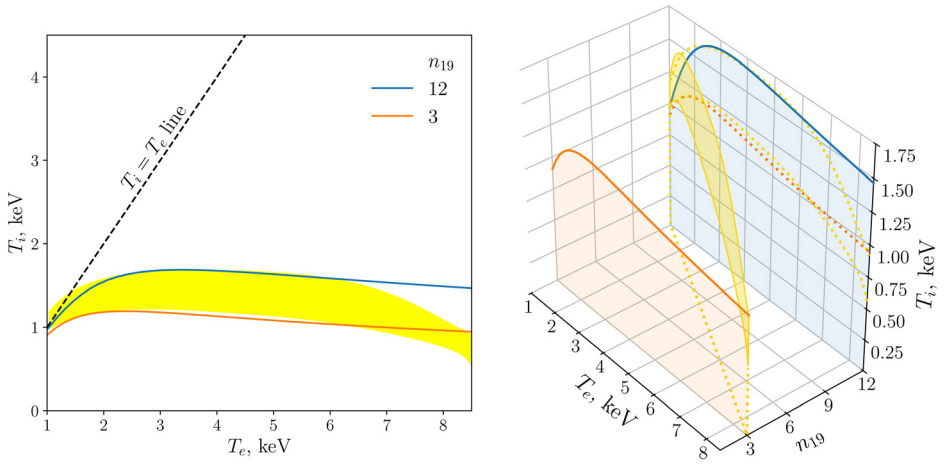

FIG. 2. T_i vs T_e in W7-X. **Left panel**: Yellow shaded area, qualitative picture of the bulk of experimental data points shown in Fig. 1(a) of Ref. 3 for discharges with various plasma densities, which match the known clamping temperature $T_i \approx 1.6$ keV. Solid lines, the functions described by Eq. (14) with $\alpha \propto T_e^2T_i^2$ for a rarefied plasma, $n_{19} = 3$ (bottom red line), and a dense plasma, $n_{19} = 12$ (top blue line). **Right panel**: same as left panel with the addition of a density axis. The diagonal location of the yellow shaded area in the density axis indicates that in experiments higher T_e is only reached at low densities. Red and yellow dotted lines on the $n_{19} = 12$ plane are, respectively, the $T_i(T_e)$ line for plasma with $n_{19} = 3$ and the bounds of the experimental data point area projected onto this plane.

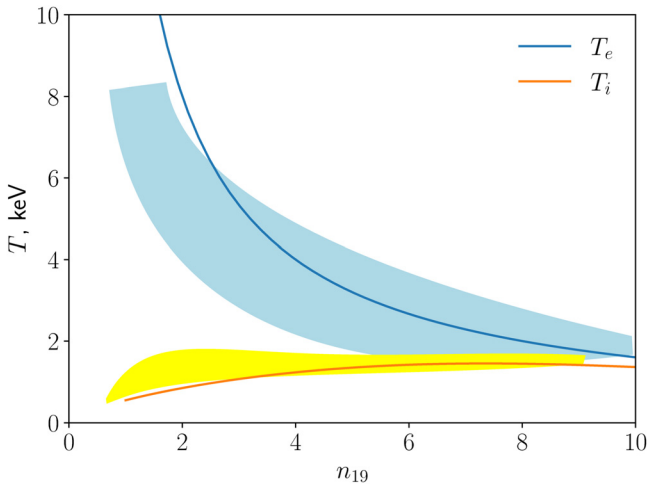

FIG. 3. T_e and T_i vs n_{19} determined by Eq. (28) with $\mathcal{P} = 7$ MW. Other parameters are the same as in Fig. 2. Yellow and blue shaded areas cover the bulk of experimental data points for, respectively, ion and electron temperatures, shown in Fig. 1(b) of Ref. 3.

ECRH, ion temperature was observed to be clamped at $T_i = 1.6$ keV, whereas T_e reached 4.1 keV. Core density was $n_{19} = 5.5$. The maximum values of the reconstructed ion temperature conductivity coefficient χ_i and of the gyro-Bohm coefficient χ_{gB} were found to be similar, although the radial dependence of χ_i and χ_{gB} did not match at all. Nevertheless, it was concluded that ITG turbulence took place in this discharge. To evaluate τ_{Ei} in this discharge, we use the expression $\tau_{Ei} = a^2/(3.84\chi_i)$,[14] which yields $\tau_{Ei} \approx 0.04$ s. We find that the LHS of Eq. (25) equals 1.7 keV, in very good agreement with observed T_i considering the approximations we take in a 0D analysis.

In discharge W7X20181016.037 (Fig. 2 of Ref. 17), there was almost the same ECRH power, but core density was raised by pellet injection to $n_{19} = 8$, with the resulting steeper density gradient presumably suppressing ITG turbulence, so that $\chi_i \ll \chi_{gB}$. In contrast to the previous discharge, no ion temperature clamping took place, with core ion temperature $T_i = 3$ keV almost reaching $T_e = 3.5$ keV. Electron temperature conductivity χ_e was three times larger than χ_i in this discharge, compared to less than 1/3 of χ_i in the preceding one. This agrees with our conclusion on the role of the ratio τ_{Ei}/τ_{Ee}, as discussed after Eq. (30). Taking $\chi_e = 0.5\,\mathrm{m}^2/\mathrm{s}$ and $\chi_i = 0.1\,\mathrm{m}^2/\mathrm{s}$ we can estimate the overall energy confinement time as $\tau_E \sim a^2/[3.84(\chi_e + \chi_i)] = 0.11$ s, which is higher than in the previous discharge by a factor of three. Evaluating the ratio of ECRH rate to the electron–ion exchange rate in this discharge [Eq. (27)], we find that this ratio was more than four times smaller in this discharge than in the preceding one where clamping was observed, although in it $p_H/[\nu_{ei}T_e(1-\Theta)]$ was only on the order of unity rather than well exceeding it. Thus, Eq. (27) is not satisfied, which breaks Eq. (30), as expected in the absence of the ion temperature clamping.

We also note that it follows from Eq. (28) that $n_e T_e/\tau_{Ee} = \mathrm{const}$ for a given ECRH power. Because normally τ_{Ee} does not depend on n_e, $T_e \propto 1/n_e$. This agrees with Fig. 1 of Ref. 3.

Finally, as we already mentioned in Sec. II B, adding NBI heating with power that is sufficiently large to break the condition Eq. (13) suppresses the clamping, which explains this effect observed in Ref. 18. One can expect that the clamping can also disappear if ICRH is added.

B. NBI heating

It is clear from Sec. II that ECRH alone cannot lead to $T_i > T_e$ (although T_i can be close to T_e) because $f_i = 0$. To reach $T_i > T_e$, a heating method is required which provides a sufficiently large fraction of energy delivered to the ions. Potentially, NBI can provide it. As shown in Appendix A, the delivered energy fraction can be described by $f_i^+ = f_i + 1.5T_i/\mathcal{E}_0$, where the first term is associated with the cooling of fast ions due to Coulomb collisions and concomitant heating of thermal ions, whereas the second term is due to the thermalized injected particles joining the bulk-ion population ($f_i = 0$ if injected ions have the energy $\mathcal{E}_0 = 1.5T_i$). In the steady state, the increase in plasma energy content due to adding thermalized ions is compensated by energy loss caused by finite particle confinement time τ_n. This implies that regimes in which the full fraction f_i^+ is relevant can only be transient, with durations on the order of τ_n. Ion heating in the stationary regime is determined by f_i given by Eqs. (A7) and (A8) or by the approximate relation (A16). In these relations, we eliminate T_i by $T_i = \Theta T_e$.

The ion power fraction is given by Eq. (12) with $\mathcal{E}_0 = 55$ keV for protons; partial powers are $\mathcal{P}_1 = 0.56\mathcal{P}$, $\mathcal{P}_2 = 0.3\mathcal{P}$, $\mathcal{P}_3 = 0.14\mathcal{P}$, and $\mathcal{E}_1 = \mathcal{E}_0$, $\mathcal{E}_2 = \mathcal{E}_0/2$, $\mathcal{E}_3 = \mathcal{E}_0/3$.

Figures 4 and 5 show the dependence of f_i and f_i^+ on T_e for various Θ. We observe that $f_i^+(T_e)$ is an increasing function which almost

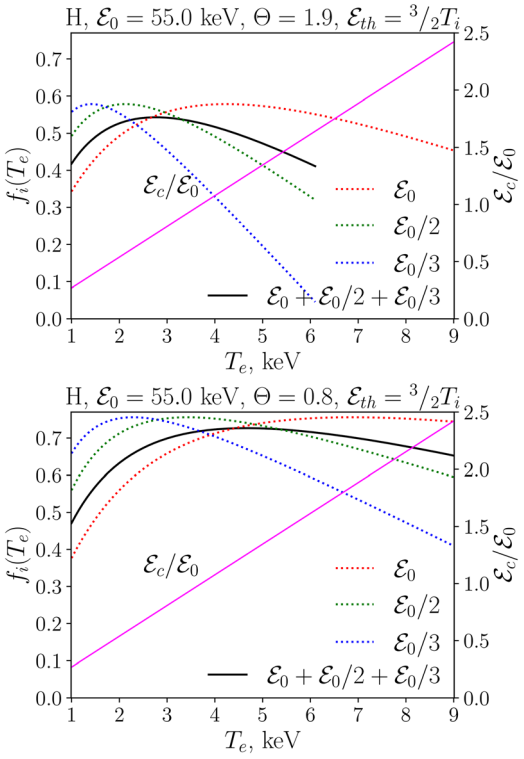

FIG. 4. f_i (black solid line), $f_i(\mathcal{E}_\sigma)$ with $\sigma = 1, 2, 3$ (dotted lines) and $\mathcal{E}_c$ for $\mathcal{E}_0$ (magenta line) vs T_e in W7-X.

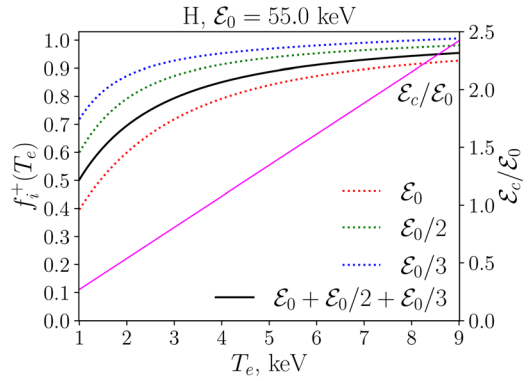

FIG. 5. The same as in Fig. 4 but for f_i^+.

does not depend on T_i or Θ. Because of this, when f_i^+ is applicable, high T_e is always favorable for scenarios transitioning to $T_i > T_e$. However, f_i depends on both T_e and Θ. It has a maximum at $T_e \sim 4$ keV when $\Theta = 1$, which shifts to lower T_e when $\Theta > 1$ and to higher T_e when $\Theta < 1$.

C. Scenarios with $T_i > T_e$ and $T_i < T_e$ in NBI-heated plasmas

A direct way to model scenarios of plasma heating is based on certain assumptions on transport coefficients of electrons and ions. Until now, these coefficients in W7-X were studied experimentally in discharges with $T_i < T_e$ only. Theoretically, various transport coefficients were obtained. They can be used for modeling particular discharges. However, they can hardly be used in general because of uncertainties associated with turbulence and other factors. Therefore, we employ another way. Prescribing plasma parameters and heating power, we consider the resulting τ_{Ei} and τ_{Ee}.

We proceed from Eqs. (1) and (2) written in the following form:

$$\tau_{Ei} = \frac{1.5\Theta}{p_H f_i/T_e - \nu_{ei}(\Theta - 1)}, \tag{45}$$

$$\tau_{Ee} = \frac{1.5}{p_H(1 - f_i)/T_e + \nu_{ei}(\Theta - 1)}, \tag{46}$$

where p_H and ν_{ei} are defined in Sec. II A.

To avoid misunderstanding, we emphasize that these relations for the energy confinement times have nothing to do with the scalings that determine the energy confinement times. They represent the confinement times required to provide a steady state energy balance of electrons and ions (similar to, e.g., the Lawson criterion).

Presumably, in the presence of the ITG turbulence, the ion energy confinement time is less than that of electrons, $\tau_{Ei} < \tau_{Ee}$, whereas $\tau_{Ei} > \tau_{Ee}$ without ITG instability. An analysis of experiments on W7-X supports this statement: it shows that $\chi_i/\chi_e \ll 1$ and $T_i \approx 3$ keV in an ECRH discharge where ITG turbulence is suppressed by pellet injection, whereas $\chi_i/\chi_e \sim 3$ with ion temperature clamped at $T_i \approx 1.6$ keV in another discharge with approximately the same heating power, see Figs. 1 and 2 in Ref. 17. This means that the intermediate case, $\tau_{Ei} = \tau_{Ee}$, represents a "border" between regions with ITG turbulence and without it in the τ_E space (when $\tau_E \propto 1/\chi$).

Thus, the ratio τ_{Ee}/τ_{Ei} is an important parameter. Introducing $\zeta \equiv \tau_{Ee}/\tau_{Ei}$ and combining Eqs. (45) and (46), we obtain the following equation:

$$\zeta = \frac{Hf_i - (\Theta - 1)}{[Hf_e + (\Theta - 1)]\Theta}, \tag{47}$$

where H is defined by Eq. (11). The formal solution of this equation with respect to Θ is

$$\Theta = 1 + \frac{1}{2}\left[-(Hf_e + 1 + \zeta^{-1}) \pm \sqrt{(Hf_e + 1 + \zeta^{-1})^2 + 4H(f_i\zeta^{-1} - f_e)}\right]. \tag{48}$$

It follows from here that a sufficient condition of $T_i > T_e$ is:

$$f_i \geq \frac{\zeta}{\zeta + 1}. \tag{49}$$

This requires $f_i \geq 0.5$ for $\zeta > 1$. On the other hand, Eq. (49) can be written as

$$\zeta = \frac{f_i}{1 - f_i}. \tag{50}$$

For prescribed Θ, this restricts electron temperature because $f_i = f_i(T_e, \Theta)$.

Taking into account the foregoing, we considered the cases with $\zeta < 1$ and $\zeta > 1$. Using Eq. (47), we calculated Θ for $\zeta = 1/3$ and $\zeta = 3$. The results are shown in Fig. 6 for plasmas with low density ($n_{19} = 1$) and high density ($n_{19} = 10$). We observe that in dense plasmas $\Theta \approx 1$, whereas in rarefied plasmas Θ can be as large as 1.9 when $\mathcal{P} = 3.5$ MW and 2.1 when $\mathcal{P} = 6.8$ MW at $T_e \sim 3$ keV. However, this is possible only if $\tau_{Ei} = 3\tau_{Ee}$, i.e., when ITG turbulence is absent. When $\tau_{Ei} = (1/3)\tau_{Ee}$, ion temperature is relatively small, $T_i < T_e$.

Figure 6, being based only on Eq. (47), is not sufficient for a final conclusion on possible temperatures. The matter is that it relies only on the ratio τ_{Ee}/τ_{Ei}, so that it is not clear whether the required magnitudes of τ_{Ee} and τ_{Ei} are realistic. Therefore, we return to Eqs. (45) and (46) to find out what values of τ_{Ee} and τ_{Ei} are required in the steady state.

The results of calculations of τ_{Ee} and τ_{Ei} are shown in Figs. 7 and 8. In addition, the gyro-Bohm time is shown in the figures, because it is often used for estimates of transport coefficients in turbulent plasmas. We define it as $\tau_g = a^2/D_g$, with

$$D_g = \frac{\rho_i^2 c_s}{a} = \frac{cT_i}{e_i B}\frac{c_s}{a\omega_B}, \tag{51}$$

where $c_s = \sqrt{T_e/M_i}$ and ω_B is the ion gyrofrequency. For hydrogen plasma and $B = 2.5$ T, τ_g reduces to

$$\tau_g = \frac{a_m^2}{T_{e,keV}^{3/2}\Theta}, \tag{52}$$

where a_m is the plasma radius in meters.

We consider first Fig. 7, top panel, relevant to a dense plasma ($n_{19} = 10$) with NBI power $\mathcal{P}_{nbi} = 3.5$ MW, which is close to the heating power in recent experiments on W7-X. In particular, Ref. 19 describes discharge W7-X 20181009.043, where NBI with power $\mathcal{P}_{nbi} = 3.6$ MW provided $T_i \approx T_e \approx 1$ keV during time interval 1–6 s.

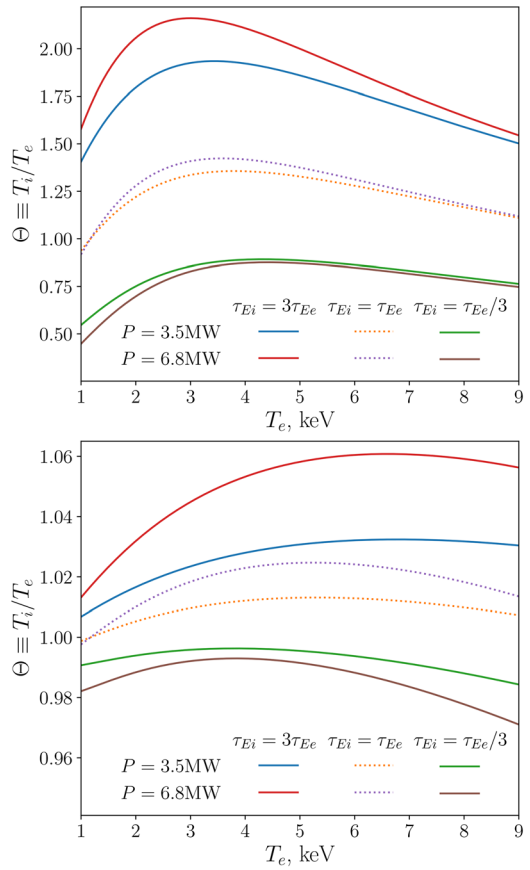

FIG. 6. The ratio T_i/T_e for $\zeta = 1/3$ (upper curves, stable ITG mode) and $\zeta = 3$ (lower curves, ITG turbulence) vs T_e: Top panel, $n_{19} = 1$; bottom panel, $n_{19} = 10$.

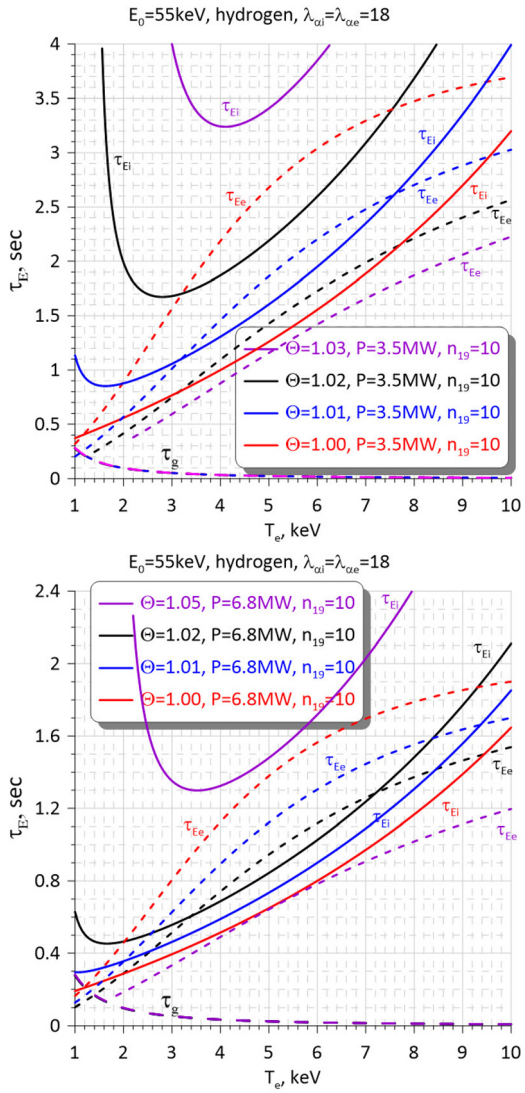

FIG. 7. Confinement times determined by Eqs. (45) and (46) in a dense plasma with $n_{19} = 10$ and the gyro-Bohm time (52): Top panel, $\mathcal{P}_{nbi} = 3.5$ MW; bottom panel, $\mathcal{P}_{nbi} = 6.8$ MW. Bold circles label the points with $\zeta = 1/3$ and $\zeta = 3$. It was assumed that $B = 2.5$ T. This figure shows dependencies required for the steady state rather than those determined by transport coefficients in plasmas [except for $\tau_g(T_e)$].

Although plasma density varied, increasing from $n_{19} \sim 1$ to $n_{19} \sim 20$ over this interval, we can evaluate the energy confinement time at $t \sim 4$ s when the diamagnetic energy $W_{dia} \approx 500$ kJ weakly changes, and $n_{19} \approx 10$, as $\tau_E = W_{dia}/\mathcal{P}_{nbi} \sim 0.14$ s (which is close to the overall energy confinement time in the ECRH discharge W7X20181016.037 where presumably ITG turbulence was suppressed, see Sec. III A). This τ_E is consistent with our Fig. 7, top panel, for $\Theta = 0.9$, $T \approx 1$ keV (bold blue circles). Increasing NBI power by a factor of two produces almost no effect on Θ, in agreement with Fig. 6, bottom panel. However, the required confinement time decreases, although it is still rather large for $T > 1$ keV. In addition, points corresponding to $\zeta = 3$ and $\zeta = 1/3$ (bold circles) shift to the left. Because of this, blue circles that corresponded to $T \approx 1$ keV at $\mathcal{P}_{nbi} = 3.5$ MW go out of range. Note that in dense plasmas, $n_{19} \gtrsim 10$, the plasma β may be unrealistically high. This is in contrast to ECRH experiments with the clamping of T_i; when $T_e = 7$ keV and $T_i \sim 1.5$ keV, β is less than that with $T_i \approx T_e \sim 7$ keV by a factor of two.

Now we proceed to a rarefied plasma. We observe in Fig. 8 that $T_i \lesssim T_e$ when electron energy is better confined than ion energy. In the contrary case, $\tau_{Ee} < \tau_{Ei}$, there are steady states with $T_i > T_e$. These results agree with Fig. 6. The magnitudes of τ_{Ee} and τ_{Ei} for which $\zeta = 1/3$ and $\zeta = 3$ are shown in Table I. It follows from Table I that when $\mathcal{P} = 3.5$ MW and $\tau_{Ee} \leq 0.15$ s (the ITG turbulence case) $T_i/T_e = 1.9/2.37$. Higher heating power, $\mathcal{P}_{nbi} = 6.8$ MW, would lead to considerably higher temperatures, $T_i/T_e = 5.98/7.47$, provided that the electron confinement time increased by a factor 1.5, otherwise the effect of the higher heating power is small. When ITG instability does not arise (e.g., due to $T_i > T_e$) ion temperature can reach 11 keV in the case of $\mathcal{P}_{nbi} = 6.8$ MW provided that $\tau_{Ei} = 0.26$ s.

Observing gyro-Bohm curves in Figs. 7 and 8, we conclude that they lie well below the τ_{Ee} and τ_{Ei} curves, except for the low-temperature region ($T_e \lesssim 2$ keV when plasma is dense, and $T_e \lesssim 1.5$ keV in a rarefied plasma). This agrees with the results shown in

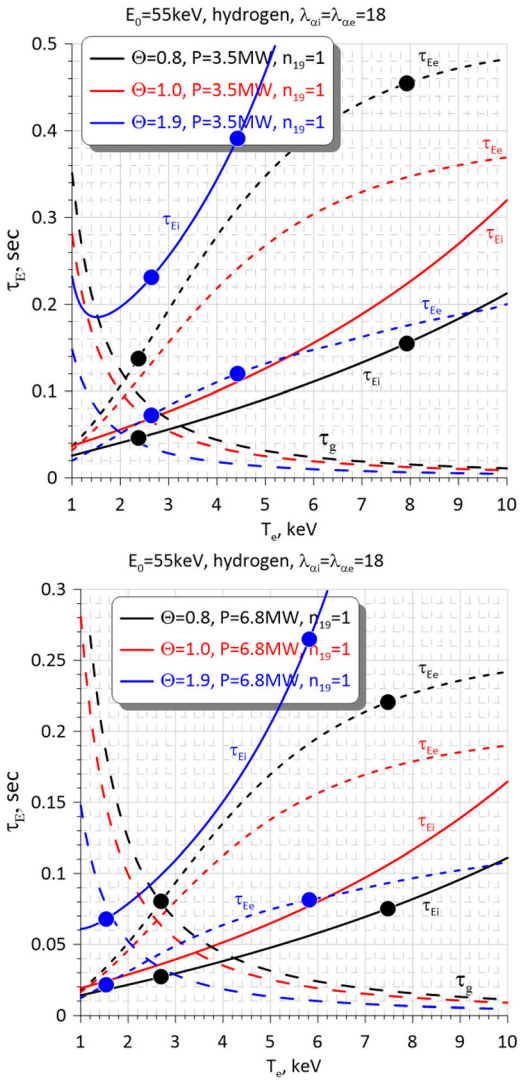

FIG. 8. Same as Fig. 7 but for a rarefied plasma with $n_{19} = 1$.

TABLE I. Plasma temperatures (T_e and T_i), confinement times (τ_{Ee} and τ_{Ei}), and ratios $\Theta \equiv T_i/T_e$, $\zeta \equiv \tau_{Ee}/\tau_{Ei}$ in plasmas with $n_{19} = 1$ for $\mathcal{P}_{nbi} = 3.5$ MW and $\mathcal{P}_{nbi} = 6.8$ MW. The shown data are true when plasma parameters provide a steady state such that ζ is either 1/3 (stable ITG mode) or 3 (ITG turbulence).

P_{MW}	τ_{Ei}, s	τ_{Ee}, s	T_i, keV	T_e, keV	Θ	ζ
3.5	0.23	0.072	5.02	2.64	1.9	1/3
	0.39	0.12	8.40	4.42		
	0.046	0.14	1.90	2.37	0.8	3
	0.16	0.45	6.34	7.93		
6.8	0.068	0.022	2.91	1.53	1.9	1/3
	0.26	0.081	11.1	5.82		
	0.027	0.081	2.16	2.70	0.8	3
	0.075	0.22	5.98	7.47		

Ref. 17, where the gyro-Bohm diffusion coefficient well exceeds the measured transport coefficients in the plasma core, but approaches or falls below the latter at the plasma periphery, where the temperature is small.

When comparing our results with previously published ones, we assumed that $\tau_E \propto 1/\chi$, which is justified when radiation in the plasma core plays a minor role. Let us see whether this assumption is justified.

The core radiation is associated mainly with electrons. One can see that τ_{Ee} is connected with $\tau_{Ee,0}$ describing the confinement time determined by the diffusivity only, as follows:

$$\tau_{Ee}^{-1} = \tau_{Ee,0}^{-1} + \frac{P_{rad}}{n_e T_e}, \tag{53}$$

where P_{rad} is the radiation power density. This can be rewritten as

$$\tau_{Ee,0} = \frac{\tau_{Ee}}{1 - \delta_{rad}}, \tag{54}$$

where

$$\delta_{rad} = \frac{P_{rad}\tau_{Ee}}{nT_e}. \tag{55}$$

When radiation is mainly due to bremsstrahlung, Eq. (55) reduces to

$$\delta_{rad} = 3.16 \times 10^{-2} Z_{eff} n_{19} T_{e,keV}^{-1/2} \tau_{Ee}, \tag{56}$$

where Z_{eff} is the effective charge number. We observe that δ_{rad} is a growing function of n_e, Z_{ef}, τ_{Ee}, but it is decreasing with T_e. For instance, when $n_{19} \sim 10$, $Z_{ef} = 1.5$ and $T_e \sim 4$ keV, $\tau_{Ee} \sim 0.1$ s, we obtain $\delta_{rad} \sim 0.02$, so that $\tau_{Ee} \approx \tau_{Ee,0}$.

One more conclusion follows from Eq. (45): it restricts plasma parameters by the inequality $p_H f_i > \nu_{ei} T_e(\Theta - 1)$, which can be considered as a restriction on the heating power, $\mathcal{P} > \mathcal{P}_{cr}$, where $\mathcal{P}_{cr} = \mathcal{P}_{cr}(T_e, \Theta, n_e)$ is determined by:

$$\mathcal{P}_{cr} = 0.24(\Theta - 1)\frac{Z_i^2 V_p n_{19}^2 \lambda_{ei}}{A_i f_i \sqrt{T_{e,keV}}} \text{MW}. \tag{57}$$

A 3D graph of $P_{cr}(n_{19}, T_e)$ for $\Theta = 1.5$ is shown in Fig. 9.

Note that steady states can be reached only if they are stable with respect to temperature fluctuations, see Appendix B. The curves for required electron and ion confinement times have $d\tau_E/dT > 0$, which means stability. On the other hand, temperature scaling is normally characterized by a negative derivative $d\tau_E/dT$. Therefore, only those τ_{Ee} and τ_{Ei} that correspond to a certain T_e can be relevant to a particular discharge.

IV. SUMMARY AND DISCUSSION

The obtained results can be summarized as follows:

(i) In plasmas with negligible ion heating by external sources (small f_i), as in the case of ECRH, the ion temperature is always capped below T_e. The capping in plasmas with anomalous ion thermal conductivity (with $\tau_{Ei} \ll \tau_{Ee}$), which can arise, for instance, when the threshold of the ITG instability is exceeded, is consistent with the main features of the ion temperature clamping observed experimentally on W7-X (see, e.g., Refs. 3 and 17): First, the capped ion temperature T_{i*} [a soft maximum of function $T_i(T_e)$ at T_{e*}] is

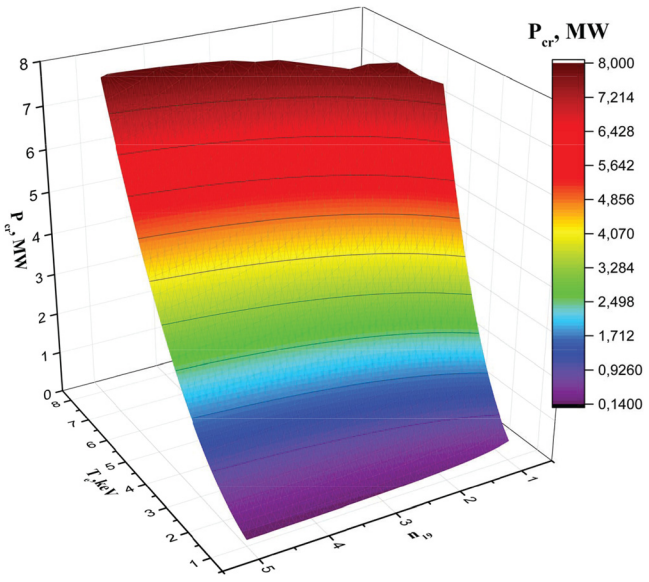

FIG. 9. Critical power $\mathcal{P}_{cr}$ (color surface) in the frame of plasma density and electron temperature for $\Theta = 1.2$ in W7-X. The magnitudes of power satisfying steady state equations are located above the surface; no steady states are possible below the surface.

below that determined by neoclassical heat transport; second, it does not depend on the heating power; third, it can be weakly dependent on the plasma density; fourth, there exists plateau-like behavior of function $T_i(T_e)$ in a region around T_{e*}, due to this $T_c \approx T_{i*}$ where T_c is a temperature at a certain specific power p_{Hc} providing $T_i \approx T_e$. Increasing p_H above p_{Hc} (by increasing the ECRH power or decreasing the plasma density) leads to growth of the electron temperature, while the ion temperature weakly changes, slowly decreasing in the region $T_e > T_{e*}$. These features of anomalous capping are demonstrated in Figs. 2 and 3.

Therefore, one can say, that *the clamping is the anomalous capping due to the ITG turbulence or another instability causing anomalous ion heat transport*.

A reservation is required: the third and fourth items suggest that the temperature dependence of τ_{Ei} is sufficiently strong (it requires $\mu + \nu + 1.5 \gg 1$ and $\nu + 1.25 > \mu^2$). It is not known what $\chi_i^{itg}(T_e, T_i)$ is in reality and whether χ_i^{itg} depends on plasma density.

It is concluded that *the clamping can disappear due to adding NBI or ICRH to ECRH*, which occurs when f_i is sufficiently large to break Eq. (13) and make the heating term $p_H f_i$ in Eq. (1) non-negligible. This can explain the absence of clamping in the W7-X experiment where ECRH was accompanied by NBI.[18] Specific relations on this issue are required for the description of experiments with mixed heating.

The obtained relations can be used for diagnostics: Knowing the clamping temperature and p_{Hc} from an experiment with $T_e \approx T_i$, one can calculate the energy confinement time $\tau_E = (\tau_{Ei}^{-1} + \tau_{Ee}^{-1})^{-1}$ by means of Eq. (31). In the case of $p_H \gg p_{Hc}$, τ_{Ei} can be determined from Eq. (25).

Estimates of the energy confinement time in several discharges in W7-X demonstrate agreement with experiment. This is an additional evidence that the conclusions based on the 0D paradigm are justified.

(ii) It is concluded that scenarios with $T_i > T_e$ are possible only when electron heating by external sources is weaker than electron cooling caused by energy loss. A hot-ion mode, i.e., a scenario with $T_i \gg T_e$, is possible when electron–ion coupling is sufficiently weak to satisfy Eqs. (38)–(42).

An important feature of NBI heating in the steady state is predicted: it is found that *the fraction of NBI power transferred to the ions (f_i) has a maximum at a certain electron temperature, T_**. In the case of W7-X, when protons with the maximum energy 55 keV are injected into hydrogen plasma, $T_* \sim 3.5$ keV at $\Theta \equiv T_i/T_e \sim 1$, being somewhat lower when $\Theta > 1$ and somewhat higher when $\Theta < 1$, see Fig. 4. The reason is that *there are two different mechanisms of plasma heating by injected ions: first, the cooling of fast NBI ions, and second, the increase in the bulk ion population by the addition of thermalized NBI ions*. In the steady state, this increase is compensated by the corresponding loss of thermal particles. Because of this, the efficiency of ion heating decreases when $T_e > T_*$. In contrast, the total fraction, $f_i^+(T_e)$, monotonically grows with T_e, approaching unity when $\mathcal{E}/\mathcal{E}_c \ll 1$ due to $\mathcal{E}_c \propto T_e$, where $\mathcal{E}_c$ is the critical energy of fast ions for which $\nu_e = \hat{\nu}_i$.

Relations connecting NBI power and plasma parameters are obtained. Confinement times $\tau_{Ee}(T_e)$ and $\tau_{Ei}(T_e)$ are calculated and shown in Figs. 7 and 8 for the range of electron temperatures $1 - 10$ keV for several values of Θ in a dense plasma ($n_{19} = 10$) and in a rarefied plasma ($n_{19} = 1$). To see which temperatures correspond to confinement times observed in W7-X experiments, it was assumed that $\zeta \equiv \tau_{Ee}/\tau_{Ei} = 3$ and $\zeta = 1/3$. This choice was made after consideration of thermal conductivity coefficients corresponding to experimental observations in W7-X reported in Ref. 17. Presumably, $\zeta = 3$ and $\zeta = 1/3$ are relevant to plasmas with and without ITG turbulence, respectively.

It is found that Θ can be as large as ~ 2 at $\zeta = 1/3$ and ~ 0.8 at $\zeta = 3$ in a rarefied plasma with $n_{19} = 1$ and $\mathcal{P}_{nbi} = 3.5$ MW or $\mathcal{P}_{nbi} = 6.8$ MW (the dependence on $\mathcal{P}_{nbi}$ was weak), see Fig. 6. In contrast, $\Theta \approx 1$ in a dense plasma, $n_{19} = 10$. These results are generic in the sense that they are determined by the ratio τ_{Ee}/τ_{Ei} but do not depend on particular magnitudes of τ_{Ee} and τ_{Ei}.

To determine whether temperatures corresponding to $\zeta = 3$ and $\zeta = 1/3$ and a prescribed Θ can be realistically achieved, τ_{Ee} and τ_{Ei} were calculated; they correspond to bold circles in Figs. 7 and 8. The ones for which τ_{Ee} and τ_{Ei} appear realistic—being close to or not drastically exceeding those already observed experimentally on W7-X—are presented in Table I. In particular, in a rarefied turbulent plasma with $\mathcal{P}_{nbi} = 6.8$ MW possible temperatures are $T_i = 5.98$ keV, $T_e = 7.47$ keV. When ITG turbulence is absent, $T_i = 11.1$ keV and $T_e = 5.82$ keV. Note that calculations were carried out for a constant power, i.e., they neglected the dependence of the absorbed power on plasma density.

Although the used magnitudes of ζ and concomitant temperatures T_e and T_i represent an example, they are sufficient to conclude that NBI heating in W7-X can result in a considerable ratio of T_i/T_e with $T_i \lesssim 10$ keV provided that the plasma is sufficiently rarefied and that the ITG threshold is not reached. In the presence of ITG turbulence, one can expect $T_i < T_e$ with T_e of several kiloelectronVolt.

Note that calculations were carried out under the assumption that all the injected power is absorbed in the plasma. This is a good approximation when plasma is sufficiently dense, $n_{19} \gtrsim 5$, but not for

more rarefied plasmas. Therefore, the temperatures shown for $n_{19} = 1$ are true for a somewhat higher injected power than that used in calculations.

The obtained relations enable one to make a quick estimate of T_i and T_e when transport coefficients are prescribed.

The results of this work are relevant to the steady state. *One can expect that transiently, the ratio of T_i/T_e can be higher than that described here because of the growth of the efficiency of ion heating due to a temporary increase in the bulk ion population, which in addition, may have a stabilizing effect on the ITG instability*. This issue deserves further study.

(iii) The work employs a paradigm that does not depend on specific stellarator configurations. For this reason, qualitative conclusions drawn in the work remain valid not only for W7-X, but also for other toroidal devices, both helical and axi-symmetric. In addition, these conclusions do not depend on the specific nature of the turbulence: they are valid whether ion thermal diffusivity is anomalous due to ITG or other instabilities such as electron temperature gradient modes (ETG) or trapped electron modes (TEM).

For the same reason, the paradigm can be applied to reactors, so that certain conclusions and recommendations can be drawn. In general, we can say, that predominant ion heating providing $T_i > T_e$ would be preferable; in this case, the fusion reactivity is maximum for prescribed β and plasma density, and the ITG threshold is largest (as discussed in Introduction). This requires optimized plasma heating by NBI and RF fields to break Eq. (13). Experiments on the EAST tokamak where the ion temperature clamping, presumably caused by ETG and TEM, was mitigated by the NBI, confirm this.[5] A similar effect was observed on W7-X,[18] where, however, turbulence was associated with ITG.

Note that in machines with the minor radius of the torus exceeding that of W7-X, the ion temperature can be as high as that in the fusion reactor due to $\tau_{Ei} \propto a^2/\chi_i$, and $T_i > T_e$ is possible (with an appropriate heating method) even in the presence of turbulence. For instance, in D-T discharges of the JET campaign DTE1, $T_i/T_e \sim 1.5$ was reached despite the fact that $\chi_i > \chi_e$ ($\chi_i \simeq 0.5\mathrm{m}^2/\mathrm{s}$ and $\chi_e \simeq 0.27\mathrm{m}^2/\mathrm{s}$); the highest $T_i \approx 17$ keV was achieved due to plasma heating by NBI and alpha particles.[24] This suggests that turbulence in fusion reactors, such as Helias and ITER, can be not as harmful. However, in any case it will require more heating power and, thus, will reduce the reactor energy gain. Therefore, the problem of suppression of the turbulence remains an important issue in reactors.

ACKNOWLEDGMENTS

The authors are grateful to M. Bozhenkov, O. Ford, and D. Moseev for discussion and valuable comments.

This work has been carried out within the framework of the EUROfusion Consortium, funded by the European Union via the Euratom Research and Training Programme (Grant Agreement No. 101052200—EUROfusion). Views and opinions expressed are, however, those of the author(s) only and do not necessarily reflect those of the European Union or the European Commission. Neither the European Union nor the European Commission can be held responsible for them.

AUTHOR DECLARATIONS

Conflict of Interest

The authors have no conflicts to disclose.

Author Contributions

Ya. I. Kolesnichenko: Conceptualization (lead); Investigation (equal); Writing – original draft (equal). **V. V. Lutsenko:** Investigation (equal); Software (equal); Validation (equal); Visualization (equal). **A. V. Tykhyy:** Investigation (equal); Software (equal); Validation (equal); Visualization (equal); Writing – original draft (equal). **W7-X Team:** Resources (supporting).

DATA AVAILABILITY

The data that support the findings of this study are available from the corresponding author upon reasonable request.

APPENDIX A: THE ENERGY RECEIVED BY THE BULK PLASMA IONS DURING COULOMB SLOWING DOWN OF A FAST ION

The energy loss of a test fast ion due to Coulomb collisions of this ion with thermal particles is described by the equation[20]

$$\dot{\mathcal{E}} = -[\nu_e + \hat{\nu}_i]\mathcal{E}. \tag{A1}$$

Here, $\mathcal{E}$ is the energy of fast ion, $\dot{\mathcal{E}} = d\mathcal{E}/dt$, ν_e and $\hat{\nu}_i \equiv \sum_i \nu_i$ (summation over bulk ion species) are collision frequencies of the energy transfer from the fast ion to thermal electrons and bulk ions, respectively,

$$\nu_j = \mathcal{E}^{-3/2}\left[(M_\alpha/M_j)\psi(x_j) - \psi'(x_j)\right]C_\alpha e_j^2 n_j \lambda_{\alpha j}, \tag{A2}$$

where

$$\begin{aligned} \psi(x_j) &= \frac{2}{\sqrt{\pi}}\int_0^{x_j} du\sqrt{u}\exp(-u), \\ \psi_j'(x_j) &= \frac{2}{\sqrt{\pi}}\sqrt{x_j}e^{-x_j}, \qquad j = e,\, i, \end{aligned} \tag{A3}$$

subscripts α, e, and i label fast ions, electrons, and bulk ions, respectively, $C_\alpha = 2^{3/2}\pi e_\alpha^2/\sqrt{M_\alpha}$, $x_j = v^2/v_{Tj}^2 = \mathcal{E}M_j/(T_j M_\alpha)$, M is the particle mass, and $\lambda_{\alpha j}$ is the Coulomb logarithm.

The slowing down time of the fast ion can be defined as the time in which its energy becomes comparable to that of thermal particles, $\mathcal{E}_{th}$. This time is determined by

$$\tau_{th} = \int_0^{\tau_{th}} tdt = \int_{\mathcal{E}_0}^{\mathcal{E}_{th}} \frac{d\mathcal{E}}{\dot{\mathcal{E}}} = \int_{\tilde{\mathcal{E}}_{th}}^{1} \frac{d\tilde{\mathcal{E}}}{(\nu_e + \hat{\nu}_i)\tilde{\mathcal{E}}}, \tag{A4}$$

where $\tilde{\mathcal{E}} = \mathcal{E}/\mathcal{E}_0$, $\tilde{\mathcal{E}}_{th} = \mathcal{E}_{th}/\mathcal{E}_0$, with $\mathcal{E}_0$ the initial energy of the fast ion.

When ions with energy $\mathcal{E}_0$ are injected into the plasma, the injected power density is $P = \mathcal{E}_0 I$, where I is the number of ions injected per second in unit volume. In addition to the power transferred to bulk plasma ions by fast ions in Coulomb collisions, bulk plasma ions receive the additional power $P_{th} = \mathcal{E}_{th} I$ representing fast ions that have slowed down to the energy $\mathcal{E}_{th} = 3T_i/2$.

Therefore, the fraction of injected power deposited to the ions can be written as

$$f_i^+ = f_i + \tilde{\mathcal{E}}_{th}, \qquad \text{and} \quad f_e = 1 - f_i, \tag{A5}$$

where f_i is associated with change of fast ion energy due to Coulomb collisions

$$f_i = \int_0^{\tau_{th}} dt \hat{\nu}_i \tilde{\mathcal{E}}. \tag{A6}$$

Because of Eq. (A1), Eq. (A6) takes the form

$$f_i = \int_{\tilde{\mathcal{E}}_{th}}^1 \frac{d\tilde{\mathcal{E}}}{1 + \nu_e/\hat{\nu}_i}, \tag{A7}$$

where

$$\frac{\nu_e}{\hat{\nu}_i} = \frac{\left[(M_\alpha/M_e)\psi(x_e) - \psi'(x_e)\right] n_e \lambda_{\alpha e}}{\sum_i \left[(M_\alpha/M_i)\psi(x_i) - \psi'(x_i)\right] Z_i^2 n_i \lambda_{\alpha i}}, \tag{A8}$$

$$x_e = \frac{M_e}{M_\alpha}\frac{\mathcal{E}_0}{T_e}\tilde{\mathcal{E}}, \qquad x_i = \frac{M_i}{M_\alpha}\frac{\mathcal{E}_0}{T_e\Theta}\tilde{\mathcal{E}}, \qquad \Theta = \frac{T_i}{T_e}. \tag{A9}$$

As expected, Eq. (A7) predicts predominant ion heating when $\nu_e \ll \hat{\nu}_i$. In the particular case of

$$\nu_e = \hat{\nu}_i, \tag{A10}$$

beam energy is deposited equally to ions and electrons. For prescribed plasma parameters, this occurs when the initial energy of fast ions equals a certain critical energy $\mathcal{E}_c$ determined by Eq. (A10), which separates the energy ranges with predominant electron and ion heating.

The relations above are exact. Below, we obtain approximate relations assuming

$$x_e \ll 1, \qquad \text{and} \quad x_i \gg 1. \tag{A11}$$

In this case, the ratio of frequencies reduces to

$$\frac{\nu_e}{\hat{\nu}_i} = \frac{\mathcal{E}^{3/2}}{\mathcal{E}_c^{3/2}}, \tag{A12}$$

with $\mathcal{E}_c$ given by

$$\frac{\mathcal{E}_c}{T_e} = 14.8\kappa, \tag{A13}$$

and

$$\kappa = A_\alpha \left(\sum_i \frac{n_i Z_i^2 \lambda_{\alpha i}}{A_i n_e \lambda_{\alpha e}} \right)^{2/3}, \tag{A14}$$

where A_i and A_α are particle mass numbers. Because of Eq. (A12), Eq. (A7) takes the form

$$f_i = \int_{\tilde{\mathcal{E}}_{th}}^1 \frac{d\tilde{\mathcal{E}}}{1 + \tilde{\mathcal{E}}^{3/2}/\tilde{\mathcal{E}}_c^{3/2}}. \tag{A15}$$

Using $\tilde{\mathcal{E}} = v^2/v_0^2 \equiv \bar{v}^2$ we obtain (cf. Refs. 21 and 22)

$$f_i = 2\int_{\bar{v}_{th}}^1 \frac{d\bar{v}\bar{v}}{1 + \bar{v}^3/\bar{v}_c{}^3} = \left[\frac{2}{\sqrt{3}} \arctan \frac{2\bar{v} - \bar{v}_c}{\sqrt{3}\bar{v}_c} - \frac{1}{3} \ln \frac{(\bar{v} + \bar{v}_c)^2}{\bar{v}^2 - \bar{v}_c\bar{v} + \bar{v}_c^2} \right]_{\bar{v}_{th}}^1 \bar{v}_c^2, \tag{A16}$$

where $\bar{v}_c = \sqrt{E_c/\mathcal{E}_0}$ and $\bar{v}_{th} = \sqrt{1.5T_i/\mathcal{E}_0}$.

It follows from Eqs. (A5) and (A16) that f_i is largest when $\mathcal{E}_0 < \mathcal{E}_c$, but it cannot reach unity ($f_i = 1$ only in the unrealistic case of $\mathcal{E}_c/\mathcal{E}_0 = \infty$). This implies that it is not possible to avoid heating the electrons, although f_e can be small. In the particular case of $\mathcal{E}_0 = \mathcal{E}_c$, $f_i < 0.738$.

Note that Eq. (A16) can be modified to approximately describe f_i^+: for this the term v^3/v_c^3 should be neglected in the integrand of Eq. (A16) and the lower limit of the integral should be taken as zero.

To evaluate the slowing down time, we take into account that due to Eq. (A11) the ion frequency $\nu_i \propto \mathcal{E}^{-3/2}$. Then, Eq. (A4) can be written as

$$\tau_{th} = \frac{1}{\hat{\nu}_{i0}} \int_{\tilde{\mathcal{E}}_{th}}^1 \frac{d\tilde{\mathcal{E}}\sqrt{\tilde{\mathcal{E}}}}{1 + \tilde{\mathcal{E}}^{3/2}/\tilde{\mathcal{E}}_c^{3/2}}. \tag{A17}$$

After calculating the integral and using the relation $\nu_i(\mathcal{E}_0)\mathcal{E}_0^{3/2}/\mathcal{E}_c^{3/2} = \nu_i(\mathcal{E}_c) = \nu_e(T_e)$ we obtain

$$\tau_{th} = \frac{2}{3\nu_e} \ln \frac{1 + (\mathcal{E}_0/\mathcal{E}_c)^{3/2}}{1 + (\mathcal{E}_{th}/\mathcal{E}_c)^{3/2}}. \tag{A18}$$

APPENDIX B: STABILITY OF STEADY STATES

Only those steady states determined by the energy balance equation can be achieved, which are stable with respect to the fluctuation of plasma parameters. This issue was considered in detail for thermonuclear burning, see, e.g., review Ref. 23. A simple but rather general stability condition can be obtained by proceeding from the following equation:

$$\frac{dT}{dt} = G(T) - \frac{T}{\tau_E(T, a)}, \tag{B1}$$

where $G(T) > 0$ describes the energy source and can include radiation losses, which do not depend on the plasma radius, and $\tau_E = a^2/\chi$, with χ the temperature conductivity coefficient. Taking $T = T^0 + \delta T$, with T^0 the steady state temperature and $\delta T = \hat{T}\exp(\gamma t)$ a small fluctuation, we obtain (the superscript "0" is omitted)

$$G(T) - \frac{T}{\tau_E} = 0, \tag{B2}$$

and

$$\gamma = \frac{dG}{dT} - \frac{1}{\tau_E} + \frac{T}{\tau_E^2}\frac{\partial \tau_E}{\partial T}. \tag{B3}$$

Here, Eq. (B2) determines steady states described by $a(T)$ and concomitant $\tau_E(T) \propto a^2(T)/\chi(T)$ (this T-dependence exists even when $\chi(T) = const$). Using this equation, we can write

$$\frac{dG}{dT} = \frac{1}{\tau_E} - \frac{T}{\tau_E^2}\frac{\partial \tau_E}{\partial T} - \frac{T}{\tau_E^2}\frac{\partial \tau_E}{\partial a}\frac{da}{dT}. \tag{B4}$$

Because of this relation, Eq. (B3) reduces to [cf. Eq. (166) in Ref. 23]

$$\gamma = -\frac{1}{\tau_E}\frac{\partial \ln \tau_E[a(T)]}{\partial \ln T}. \tag{B5}$$

It follows that only steady states with $d\tau_E/dT > 0$ are stable and can take place, unless a feedback stabilization is employed. In order to avoid misunderstanding, we note that temperature dependence of steady states determined by $\tau_E(T)$ has nothing to do with the T-scaling of energy confinement time.

REFERENCES

[1]C. D. Beidler, H. M. Smith, A. Alonso, T. Andreeva, J. Baldzuhn, M. N. A. Beurskens, M. Borchardt, S. A. Bozhenkov, K. J. Brunner, H. Damm, M. Drevlak, O. P. Ford, G. Fuchert, J. Geiger, P. Helander, U. Hergenhahn, M. Hirsch, U. Höfel, Ye. O. Kazakov, R. Kleiber, M. Krychowiak, S. Kwak, A. Langenberg, H. P. Laqua, U. Neuner, N. A. Pablant, E. Pasch, A. Pavone, T. S. Pedersen, K. Rahbarnia, J. Schilling, E. R. Scott, T. Stange, J. Svensson, H. Thomsen, Y. Turkin, F. Warmer, R. C. Wolf, D. Zhang, and W7-X Team, Nature **596**(12), 221 (2021).

[2]T. Klinger, T. Andreeva, S. Bozhenkov, C. Brandt, R. Burhenn, B. Buttenschön, G. Fuchert, B. Geiger, O. Grulke, H. P. Laqua, N. Pablant, K. Rahbarnia, T. Stange, A. von Stechow, N. Tamura, H. Thomsen, Y. Turkin, and T. Wegner, Nucl. Fusion **59**(11), 112004 (2019).

[3]M. N. A. Beurskens, S. A. Bozhenkov, O. Ford, P. Xanthopoulos, A. Zocco, Y. Turkin, A. Alonso, C. Beidler, I. Calvo, D. Carralero, T. Estrada, G. Fuchert, O. Grulke, M. Hirsch, K. Ida, M. Jakubowski, C. Killer, M. Krychowiak, S. Kwak, S. Lazerson, A. Langenberg, R. Lunsford, N. Pablant, E. Pasch, A. Pavone, F. Reimold, Th. Romba, A. von Stechow, H. M. Smith, T. Windisch, M. Yoshinuma, D. Zhang, R. C. Wolf, and W7-X Team, Nucl. Fusion **61**(11), 116072 (2021).

[4]J. A. Alcusón, P. Xanthopoulos, G. G. Plunk, P. Helander, F. Wilms, Y. Turkin, A. von Stechow, and O. Grulke, Plasma Phys. Controlled Fusion **62**(3), 035005 (2020).

[5]J. Liu, Q. Zang, Y. Liang, J. Chen, X. Wu, A. Knieps, J. Hu, Y. Jin, B. Zhang, Y. Chu, H. Liu, B. Lyu, Y. Duan, M. Li, Y. Chen, X. Gong, and EAST Team, Plasma Sci. Technol. **26**, 045103 (2024).

[6]M. N. A. Beurskens, C. Angioni, S. Bozhenkov, O. Ford, C. K. Kiefer, P. Xanthopoulos, Y. Turkin, J. A. Alcusón, J. P. Baehner, C. Beidler, G. Birkenmeier, E. Fable, G. Fuchert, B. Geiger, O. Grulke, M. Hirsch, M. Jakubowski, H. P. Laqua, A. Langenberg, S. Lazerson, N. Pablant, M. Reisner, P. Schneider, E. R. Scott, T. Stange, A. von Stechow, J. Stober, U. Stroth, T. Wegner, G. Weir, D. Zhang, A. Zocco, R. C. Wolf, H. Zohm, W7-X Team, ASDEX Upgrade Team, and EUROfusion MST1 Team, Nucl. Fusion **62**, 016015 (2022).

[7]W. Horton, Rev. Mod. Phys. **71**(3), 735 (1999).

[8]Ya. I. Kolesnichenko, B. S. Lepiavko, and Yu. V. Yakovenko, Plasma Phys. Controlled Fusion **54**, 105001 (2012).

[9]K. Ida, Y. Sakamoto, M. Yoshinuma, H. Takenaga, K. Nagaoka, N. Hayashi, N. Oyama, M. Osakabe, M. Yokoyama, H. Funaba, N. Tamura, K. Tanaka, Y. Takeiri, K. Ikeda, K. Tsumori, O. Kaneko, K. Itoh, S. Inagaki, T. Kobuchi, A. Isayama, T. Suzuki, T. Fujita, G. Matsunaga, K. Shinohara, Y. Koide, M. Yoshida, S. Ide, Y. Kamada, LHD Experiment Group, and JT-60 Team, Nucl. Fusion **49**, 095024 (2009).

[10]M. Osakabe, H. Takahashi, H. Yamada, K. Tanaka, T. Kobayashi, K. Ida, S. Ohdachi, J. Varela, K. Ogawa, M. Kobayashi, K. Tsumori, K. Ikeda, S. Masuzaki, M. Tanaka, M. Nakata, S. Murakami, S. Inagaki, K. Mukai, M. Sakamoto, K. Nagasaki, Y. Suzuki, M. Isobe, T. Morisaki, and LHD Experiment Group, Nucl. Fusion **62**, 042019 (2022).

[11]Y. F. He, J. P. Qian, J. G. Li, P. Li, X. Z. Gong, B. Zhang, J. Y. Zhang, J. L. Chen, C. Bae, M. Q. Wu, X. D. Yang, T. Q. Jia, G. S. Li, Y. F. Jin, Z. C. Lin, S. Y. Fu, G. L. Lin, Q. Zang, G. Q. Zhong, S. X. Wang, X. Li, and J. Huang, Nucl. Fusion **64**, 076064 (2024).

[12]D. K. Mansfield, J. D. Strachan, M. G. Bell, S. D. Scott, R. Budny, E. S. Marmar, J. A. Snipes, J. L. Terry, S. Batha, R. E. Bell, M. Bitter, C. E. Bush, Z. Chang, D. S. Darrow, D. Ernst, E. Fredrickson, B. Grek, H. W. Herrmann, K. W. Hill, A. Janos, D. L. Jassby, F. C. Jobes, D. W. Johnson, L. C. Johnson, F. W. Levinton, D. R. Mikkelsen, D. Mueller, D. K. Owens, H. Park, A. T. Ramsey, A. L. Roquemore, C. H. Skinner, T. Stevenson, B. C. Stratton, E. Synakowski, G. Taylor, A. von Halle, S. von Goeler, K. L. Wong, and S. J. Zweben, Phys. Plasmas **2**(11), 4252 (1995).

[13]R. J. Hawryluk, V. Arunasalam, C. W. Barnes, M. Beer, M. Bell, R. Bell, H. Biglari, M. Bitter, R. Boivin, N. L. Bretz, R. Budny, C. E. Bush, C. Z. Cheng, T. K. Chu, S. A. Cohen, S. Cowley, P. C. Efthimion, R. J. Fonck, E. Fredrickson, H. P. Furth, R. J. Goldston, G. Greene, B. Grek, L. R. Grisham, G. Hammett, W. Heidbrink, K. W. Hill, J. Hosea, R. A. Hulse, H. Hsuan, A. Janos, D. Jassby, F. C. Jobes, D. W. Johnson, L. C. Johnson, J. Kesner, C. Kieras-Phillips, S. J. Kilpatrick, H. Kugel, P. H. La Marche, B. LeBlanc, D. M. Manos, D. K. Mansfield, E. S. Marmar, E. Mazzucato, M. P. McCarthy, M. Mauel, D. C. McCune, K. M. McGuire, D. M. Meade, S. S. Medley, D. R. Mikkelsen, D. Monticello, R. Motley, D. Mueller, Y. Nagayama, G. A. Navratil, R. Nazikian, D. K. Owens, H. Park, W. Park, S. Paul, F. Perkins, S. Pitcher, A. T. Ramsey, M. H. Redi, G. Rewoldt, D. Roberts, A. L. Roquemore, P. H. Rutherford, S. Sabbagh, G. Schilling, J. Schivell, G. L. Schmidt, S. D. Scott, J. Snipes, J. Stevens, B. C. Stratton, W. Stodiek, E. Synakowski, Y. Takase, W. Tang, G. Taylor, J. Terry, J. R. Timberlake, H. H. Towner, M. Ulrickson, S. von Goeler, R. Wieland, M. Williams, J. R. Wilson, K. L. Wong, M. Yamada, S. Yoshikawa, K. M. Young, M. C. Zarnstorff, and S. J. Zweben, Plasma Phys. Controlled Fusion **33**(13), 1509 (1991).

[14]K. Miyamoto, "Fundamentals of plasma physics and controlled fusion," Report No. NIFS-PROC-48, 2000.

[15]J. Ramos, Phys. Plasmas **12**, 112301 (2005).

[16]A. B. Navarro, A. Di Siena, J. L. Velasco, F. Wilms, G. Merlo, T. Windisch, L. L. LoDestro, J. B. Parker, and F. Jenko, Nucl. Fusion **63**, 054003 (2023).

[17]M. Wappl, S. A. Bozhenkov, T. Andreeva, S. Bannmann, H. M. Smith, R. C. Wolf, and W7-X Team, Plasma Phys. Controlled Fusion **67**(7), 075025 (2025).

[18]A. Langenberg, F. Warmer, G. Fuchert, O. Ford, S. Bozhenkov, T. Andreeva, S. Lazerson, N. A. Pablant, T. Gonda, M. N. A. Beurskens, K.-J. Brunner, B. Buttenschön, A. Dinklage, D. Hartmann, J. Knauer, O. Marchuk, E. Pasch, F. Reimold, T. Stange, T. Wegner, O. Grulke, R. C. Wolf, and W7-X Team, Phys. Plasmas **31**, 052502 (2024).

[19]S. A. Lazerson, Y. Turkin, H. Smith, S. Äkäslompolo, M. Drevlak, D. Pfefferlé, S. Bozhenkov, O. Ford, N. Rust, P. McNeely, D. Hartmann, K. Rahbarnia, T. Andreeva, J. Schilling, C. Brandt, U. Neuner, H. Thomsen, R. C. Wolf, and W7-X Team, in 47th EPS Conference on Plasma Physics (2021).

[20]A. S. Richardson, "2019 NRL plasma formulary," Technical report, 2019.

[21]D. J. Sigmar and G. Joyce, Nucl. Fusion **11**, 447 (1971).

[22]T. H. Stix, Plasma Phys. **14**, 367–384 (1972).

[23]Ya. I. Kolesnichenko, Nucl. Fusion **20**, 727 (1980).

[24]Ya. I. Kolesnichenko, V. V. Lutsenko, M. H. Tyshchenko, H. Weisen, Yu. V. Yakovenko, and JET Contributors, Nucl. Fusion **58**, 076012 (2018).